Structural, electronic, optical and elastic properties of Mg_3TH_7 (T=Mn, Tc and Re) complex hydrides: First-principles calculations

K. Benyelloul [1*] , Y. Bouhadda [1], M. Bououdina [3,4]
N. Fenineche [5], H. Aourag [2] and H. Faraoun [2]

[1] Unité de Recherche Appliquée en Energies Renouvelables, URAER
Centre de Développement des Energies Renouvelables, CDER
47133, Ghardaïa, Algeria

[2] Department of Physics, Tlemcen University, 13000 Algeria

[3] Department of Physics, College of Science
University of Bahrain, P.O. Box 32038, Bahrain

[4] Nanotechnology Centre, University of Bahrain
P.O. Box 32038, Bahrain

[5] IRTES-LERMPS, UTBM, Site de Montbéliard
90010 Belfort Cedex, France

(reçu le 20 Novembre 2015 – accepté le 23 Décembre 2015)

Abstract - *The structural, electronic, optical and elastic properties of Mg_3TH_7 (T=Mn, Tc, Re) complex hydrides have been investigated by using the density functional theory 'DFT' within the generalized gradient approximation 'GGA' parameterized by the Perdew, Burke and Ernzerhof 'PBE'. The optimized lattice constants, atomic positions and interatomic distance are in good agreement with both theoretical results and experimental data available in the literature. Band structure, densities of states 'DOS', optical properties, and elastic constants have been calculated. The obtained results of elastic properties were compared with those of the simplest Mg-based hydride MgH_2. More importantly, it is found that, the energy band gap is highly augmented when Mn atom is replaced by Re, but it is less pronounced when Re atom is replaced by Tc. From elastic constants calculations, it is noted that MgH_2, Mg_3MnH_7, Mg_3TcH_7 and Mg_3ReH_7 compounds are mechanically stable and are brittle. In addition, the polycrystalline elastic properties such as bulk modulus, shear modulus, Young modulus and Poisson's ratio were also determined by the Voigt-Reuss-Hill, 'VRH' approximation. It was found that the bulk modulus of complex hydrides Mg_3TH_7 (T=Mn, Tc and Re) are higher than that of MgH_2 and increases with increasing atomic number of element (Mn, Tc, Re) in the sequence (B) Mg_3MnH_7 < (B) Mg_3TcH_7 < (B) Mg_3ReH_7. The shear anisotropy, linear bulk modulus and percentage anisotropy in compressibility and shear were also determined and discussed in details. Finally, Debye temperatures were calculated and discussed.*

Résumé – *Les propriétés structurelle, électronique, optique et élastique de l'hybride complexe Mg_3TH_7 (T=Mn, Tc, Re) ont été étudiées en utilisant la théorie de la densité fonctionnelle 'DFT' et la technique d'approximation du gradient généralisé 'CGA' paramétrée par Perdew, Burke et Ernzerhof 'PBE'. Les constantes optimisées du réseau, les positions atomiques et intra-atomiques sont en concordance avec les résultats théoriques et les données expérimentales disponibles dans les publications. La structure de la bande, les états de densité 'DOS', les propriétés optiques et les constantes élastiques ont été calculées. Les résultats obtenus sur l'élasticité ont été comparés avec celle du plus simple Mg hybride MgH_2. D'autant plus, il a été découvert que, le différentiel énergétique de la bande augmente quand l'atome du Mn est remplacé par le Re, et est moins important que quand l'atome du Re est remplacé par le Tc. A partir des calculs d'élasticité des constantes, on note que les composants du MgH_2, Mg_3MnH_7, Mg_3TcH_7 et Mg_3ReH_7 sont mécaniquement stables, mais fragiles. Plus encore, les propriétés élastiques des polycristallins tels que les modules de masse, les modules de cisaillement, le module de Young et le ratio de Poisson ont été déterminéz par Voigt-Reuss-Hill, technique*

* Benyelloul.kamel@yahoo.fr

d'approximation 'VRH'. On a aussi trouvé que les modules de masse des hybrides complexes Mg_3TH_7 (T=Mn, Tc et Re) sont plus importants que ceux du MgH_2 et progressent avec l'augmentation du nombre atomique de l'élément (Mn, Tc, Re) dans la séquence (B) Mg_3MnH_7 < (B) Mg_3TcH_7 < (B) Mg_3ReH_7. Le cisaillement anisotropique, les modules linéaires de masse et le pourcentage anisotropique dans la capacité de compression et de cisaillement ont été eux aussi déterminés et discutés en détail. Enfin, les températures de Debye ont été mesurées et discutées.

Keywords: Complex hydrides - Elastic properties - Electronic structure - Optical properties - First-principles calculations.

1. INTRODUCTION

In the recent decades, the research and the development of new hydrogen storage materials opened new possibilities for industrials. On the other hand, the major challenges in solid-state hydrogen storage, with particular reference to fuel cells and rechargeable batteries, are improved energy storage density, faster kinetics and better cycle life, by using readily available elements at reasonable cost [1, 2]. The ternary complex transition hydrides are considered to be very attractive candidates and received significant attention as hydrogen storage materials. These compounds show higher capability of hydrogen storage at volume densities than those of compressed gaseous and liquid hydrogen, and they have hydrogen decomposition in range of 100-400°C at 1 bar H2 pressure [3]. Recently, the ternary Mn-based hydrides are elaborated by Bronger's research group [4]. Bortz *et al.*, [5] have prepared a new manganese ternary hydride, Mg_3MnH_7, which showed excellent hydrogen storage capacity of about 5.2 Wt% H2 compared to MgH_2 (7.1 Wt% H_2). The Mg_3MnH_7, has a relatively low desorption temperature of 250°C (350°C for MgH_2) [6]. The second hydrides, Mg_3ReH_7 which is iso-structural to Mg_3MnH_7, was synthesized and studied by B. Huang *et al.*, [7]. These compounds have demonstrated the most promising properties due to their crystal chemistry. With the occurrence of the first hydrido-Mn and hydrido–Re complex ions $[MnH_6]^{5-}$ and $[ReH_6]^{5-}$, respectively [8]. Indeed, Matar *et al.*, [8] have investigated the electronic structure and bonding of three different complex hydrides Mg_3MnH_7, Mg_3ReH_7 and Mg_3TcH_7 from pseudo-potentials and all-electrons computations within DFT. They have shown that both Mg_3MnH_7 and Mg_3ReH_7 have desorption energies within the range of MgH_2 and higher than covalent-like hydrogenated intermetallic compounds. The complex hydrides Mg_3MnH_7 and Mg_3ReH_7 compounds crystallize in the hexagonal *$P6_3/mmc$* (space group 194) [5, 7] shown in figure 1**a-**, where Mn and Re atoms occupy the *2a* Wyckoff sites, while the atoms occupying the *4f*, *2b*, *12k* and *2c* Wyckoff sites will be referred hereafter as $Mg_{(1)}$, $Mg_{(2)}$, $H_{(1)}$ and $H_{(2)}$, respectively. For T=Tc, a hypothetic hexagonal structure was included, the starting data were taken as those of T=Mn. The MgH_2 crystallizes in a rutile (tetragonal) phase which corresponds to *$P4_2/mnm$* (space group 136) [9] shown in figure 1**b-**, where Mg atoms occupy the *2a* Wyckoff sites, while H occupy the *4f* Wyckoff sites.

In this paper, the first principles was carried out to investigate the structural, electronic, optical and elastic properties of hexagonal ternary complex hydrides Mg_3TH_7 (T=Mn, Tc and Re) compounds. The structural and electronic properties calculations are compared comprehensively to the available experimental and theoretical literature [5, 7, 8, 10]. To the best of our knowledge there are no theoretical investigation on the elastic and optical properties of Mg_3MnH_7, Mg_3ReH_7 and Mg_3TcH_7 ternary complex hydrides. Thereby, elastic and mechanical properties calculations were compared to the simplest Mg-based hydride MgH_2. It is well known that the elastic properties, optical properties and electronic structure of complex hydrides play an important role in many applications related to the mechanical properties of materials and optoelectronic technology [11]. The

paper is organized as follows. In section 2, details of the theory and computational are presented. The most relevant results obtained are presented and discussed in section 3. Finally, a conclusion of the present work is given in section 4.

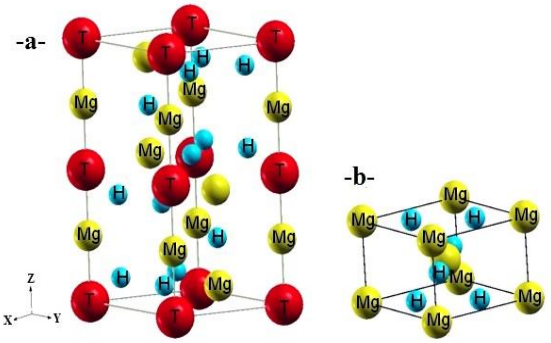

Fig. 1: The hexagonal structure of Mg_3TH_7 (T=Mn, Tc, Re) **-a-** and the tetragonal structure of MgH_2 -b-

2. COMPUTATIONAL DETAILS

The electronic structure calculations are based on the density functional theory 'DFT' [12] as implemented in the Vienna Ab-initio Simulation Package 'VASP' [13, 14], using the projector augmented wave 'PAW' method [15]. The exchange-correlation energy functional was treated by the generalized gradient approximation 'GGA' parameterized by the Perdew, Burke and Ernzerhof, 'PBE' [16]. The cut-off energy for the all calculations of plane wave was chosen as 450 eV. The linear tetrahedron method with Blöchl corrections [17] as well as a Methfessel *et al.*, [18] scheme were applied for both geometry relaxation and total energy calculations. The Brillouin zone integration used Gamma centered Monkhorst-Pack grids [19] of 5×5×4 and 7×7×9 for optimizing geometry and calculating elastic constants for hexagonal structure of ternary complex hydrides Mg_3TH T=Mn, Tc, Re) and rutile phase of magnesium hydrides MgH_2 respectively. The density of states 'DOS', band structure and optical properties calculations for Mg_3TH_7 (T=Mn, Tc and Re) were performed with 9×9×7 ^{k}-point mesh.

3. RESULTS AND DISCUSSIONS

3.1 Structural properties

The optimized atomic coordinates as well as the corresponding experimental values for each Mg_3TH_7 (T=Mn, Tc, Re) and MgH_2 compound are shown in **Table 1**. It can be seen that results are in good agreement with experimental and theoretical values [5, 7-9]. The calculated equilibrium volume cell (V_0) and bulk modulus (B) of MgH_2, Mg_3TH_7 (T=Mn, Tc, Re) are extracted by fitting the total energy as a function of volumes [20], the plot of volume versus energy is shown in figure 2. The optimized lattice parameters (in Å), ratio (c / a), volume cell V_0 (in $Å^3$), bond length $d_{T-H(1)}$ (T=Mn, Tc and Re), $d_{Mg1-H(2)}$ (in Å), bulk modulus B (in GPa) and its derivative (B') for MgH_2, Mg_3MnH_7, Mg_3TcH_7 and Mg_3ReH_7 are determined and reported in **Table 2**.

For MgH_3, the optimized lattice parameters ($a = 4.5188\,A°$, $c = 3.0133\,A°$) are consistent with the experimental unit-cell values ($a = 4.5168\,A°$, $c = 3.0205\,A°$) [9].

For Mg_3MnH_7, the optimized lattice parameters $a = 4.6917\,A°$ and $c = 10.2482\,A°$, exhibit a slight deviations 0.367 % less than experimental unit-cell parameters $a = 4.709\,A°$ and $c = 10.268\,A°$ [5].

In case of Mg_3ReH_7, the optimized lattice parameters are $a = 4.8501A°$, $c = 10.6322\,A°$ a deviations from the experimental unit-cell parameters a and c are observed and are given by -0.08 % and 0.59 % respectively, which are in accord with experimental data [7].

For Mg_3TcH_7 compounds the calculated equilibrium lattice parameters (a , c) are in good agreement with those reported by theoretical results [8]. The calculated bond length $d_{Mn-H(1)}$, $d_{Mg(1)-H(2)}$, in Mg_3MnH_7 hydrides and $d_{Re-H(1)}$, $d_{Mg(1)-H(2)}$ in Mg_3ReH_7 hydrides are respectively 1.626 A°, 1.887 A°, 1.762 A° and 1.92 A° and are in accord with experimental and theoretical values [5, 7, 8].

For Mg_3TcH_7 compounds the calculated bond length $d_{Tc-H(1)} = 1.76\,A°$ and $d_{Mg(1)-H(2)} = 1.907$ A° are in good agreement with those reported by theoretical results [8]. The obtained results of bulk modulus for MgH_2 ($B = 53.26\,GPa$) is in good agreement with the theoretical value [21-23]. In addition, the calculated bulk moduli for Mg_3MnH_7, Mg_3TcH_7 and Mg_3ReH_7 are 83.81 GPa, 90.42 GPa and 93.87 GPa, respectively. It was found that these values are greater than MgH_2 compounds and increase with increasing the atomic number of the element (Mn, Tc, Re) in the sequence $(B)\ Mg_3MnH_7 < (B)\ Mg_3TcH_7 < (B)\ Mg_3ReH_7$ (see figure 3-**a**-). Since, no experimental data on bulk modulus were found. Therefore, the theoretical prediction of B values should be of interest in future investigations.

Table 1: The optimized atomic coordinates of MgH_2 and Mg_3TH_7 (T=Mn, Tc, Re) hydrides

Compounds	Space group	Atom	Site	Present work			Expt.		
				x	*y*	*z*	*x*	*y*	*z*
MgH_2	136	Mg	2*a*	0	0	0	0	0	0
		H	4*f*	0.3045	0.3045	0	0.304[a]	0.304[a]	0[a]
Mg_3MnH_7	194	Mn	2*a*	0	0	0	0	0	0
		Mg(1)	4*f*	1/3	2/3	0.06569	1/3[b]	2/3[b]	0.0678[b]
									0.066[d]
		Mg(2)	2*b*	0	0	1/4	0[b]	0[b]	1/4
		H(1)	12*k*	0.1638	0.3267	0.5931	0.1622[b]	0.3244[b]	0.593[b]
							0.164[d]		0.593[d]
		H(2)	2*c*	1/3	2/3	1/4	1/3[b]	2/3[b]	1/4[b]
Mg_3TcH_7	194	Tc	2*a*	0	0	0	0	0	0
		Mg(1)	4*f*	1/3	2/3	0.0684	1/3	2/3	0.068[d]
		Mg(2)	2*b*	0	0	1/4	0	0	1/4
		H(1)	12*k*	0.172	0.3401	0.599	0.170[d]		0.599[d]
		H(2)	2*c*	1/3	2/3	1/4			
Mg_3ReH_7	194	Re	2*a*	0	0	0	0[c]	0[c]	0[c]
		Mg(1)	4*f*	1/3	2/3	0.06857	1/3[c]	2/3[c]	0.0702[c]
									0.069[d]
		Mg(2)	2*b*	0	0	1/4	0[c]	0[c]	1/4[c]
		H(1)	12*k*	0.1691	0.3382	0.5979	0.1656[c]	0.3312[c]	0.5962[c]
							0.169[d]		0.598[d]
		H(2)	2*c*	1/3	2/3	1/4	1/3[c]	2/3[c]	1/4[c]

[a] Ref. [9], [b] Ref. [5], [c] Ref. [7], [d] Ref [8]

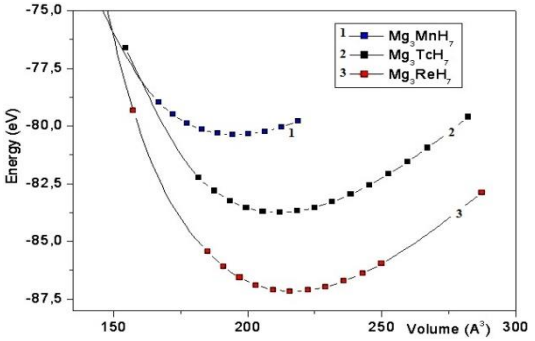

Fig. 2: Energy as a function of volume for Mg_3MnH_7 , Mg_3TcH_7 and Mg_3ReH_7

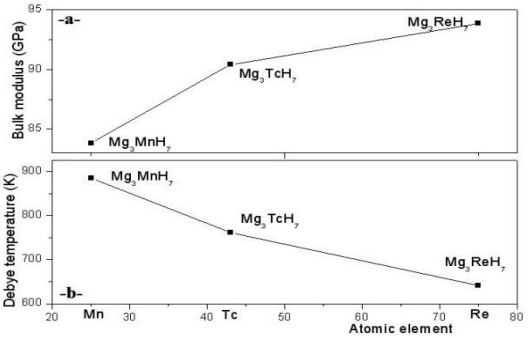

Fig. 3: Variation of the bulk modulus of Mg_3TH_7 (T=Mn, Tc, Re) as a function of atomic element a) and the variation of Debye temperature of Mg_3TH_7 (T=Mn, Tc, Re) as a function of atomic element b).

Table 2: The calculated lattice parameters (a , c) (in Å), c / a , equilibrium volume V_0 (in Å^3), bond length (in Å), bulk modulus B (in GPa) and derivative of bulk modulus B' of MgH_2 and Mg_3TH_7 (T=Mn, Tc, Re) hydrides

Parameter	MgH_2	Mg_3MnH_7	Mg_3TcH_7	Mg_3ReH_7
a	4.5188	4.6917	4.810	4.8501
	4.5168[a]	4.7090[b]		4.8540[c]
		4.670[g]	4.822[g]	4.835[g]
c	3.0133	10.2482	10.505	10.6322
	3.0205[a]	10.2860[b]		10.5690[c]
		10.250[g]	10.488[g]	10.574[g]
c/a		2.1843	2.184	2.1921
		2.1840[b]		2.1780[c]
		2.196[g]	2.175[g]	2.187[g]
V_0		195.36	210.48	216.59
$d_{T\text{-}H(1)}$		1.626	1.76	1.762
		1.63[b]		1.724[c]
		1.63[g]	1.75[g]	1.76[g]
$d_{Mg1\text{-}H(2)}$		1.887	1.907	1.92
		1.87[b]		1.901[c]
		1.88[g]	1.91[g]	1.92[g]
B	53.26 45[d] 55[e] 50[f]	83.81	90.42	93.87
B'	3.74 3.35[d]	3.76	3.80	3.83

[a] Ref.[9], [b] Ref.[5], [c] Ref.[7], [d] Ref.[22], [e] Ref.[23], [f] Ref.[21], [g] Ref.[8]

3.2 Electronic properties

The calculated band structures in hexagonal phases for Mg_3MnH_7, Mg_3ReH_7 and Mg_3cH_7 along the following special high-symmetry point in the Brillouin zone: A (0,0,1/2), H (1/3,1/3,1/2), K (1/3,1/3,0), Gamma (G) (0,0,0), M (1/2,0,0) and L (1/2,0,1/2) are displayed in figure 4-**a-**, 4-**b-** and 4-**c-** respectively. The top of valence band is taken as the zero energy level. It is clear that these materials are direct band gap as it occurs along $M \rightarrow M$ between the maximum of the valence band and minimum of the conduction band. The calculated band-gap energy for Mg_3MnH_7, Mg_3ReH_7 and Mg_3TcH_7 are 1.65 eV, 2.68 eV and 2.66 eV respectively. We can notice that the band gap energy is significantly augmented when Mn atom is replaced by Re, but it is less pronounced when Re atom is replaced by Tc. The obtained densities of states (DOS) and partial densities of states (PDOS) for Mg_3MnH_7, Mg_3ReH_7 and Mg_3TcH_7 are shown in figure 5-**a-**, 5-**b-** and 5-**c-**, respectively. From figure 5-**a-**, it can be seen that in low energy level ranging between -6.5 eV and -2.3 eV indicates that Mg_3MnH_7 exhibits strong hybridization mainly between Mn-d state and H(1), as well as smaller bonding between H(2) and Mg(1)-s state. Whilst, the upper valence states situated between -1 eV to Fermi level (E_F) is dominated by the Mn-d state. In case of Mg_3ReH_7 (figure 5-**b-**) the Re-d state and H(1) exhibit strong hybridization, as well as smaller bonding between Mg(1)-s and H(2) in the region between -6 eV and -1.85 eV. In the valence bands just below Fermi level ranging from 0 to -1.40 eV is dominated by Re-d state. Finally, the compounds Mg_3TcH_7 (figure 5-**c-**), exhibit strong hybridization between Tc-d state and H(1), as well as smaller bonding between Mg(1)-s and H(2) in the region from -5.10 eV to -1.50 eV, but the section between -1.20 eV and 0 below Fermi level, is dominated by Tc-d state.

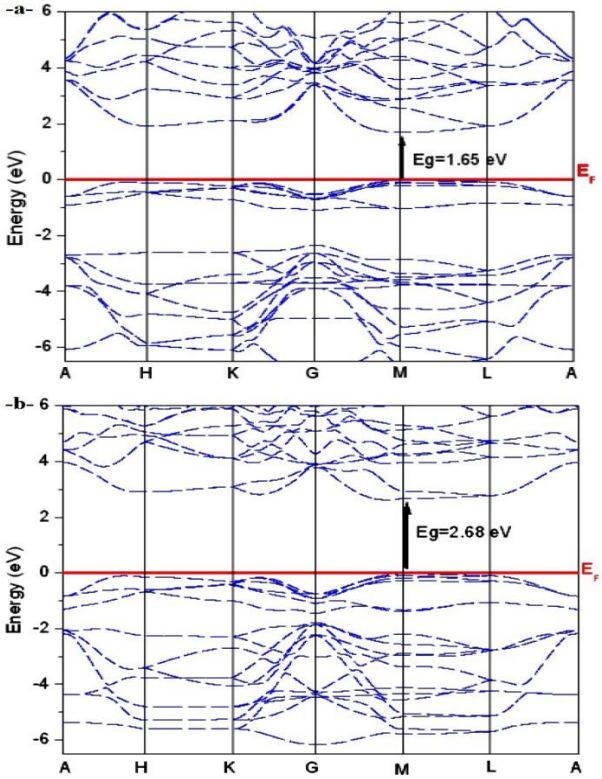

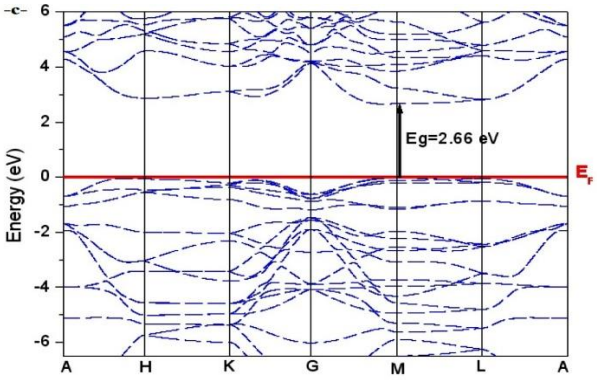

Fig. 4: Band structure of Mg_3MnH_7 -a, Mg_3ReH7 **-b** and Mg_3TcH_7 -c along with the high symmetry point of the Brillouin zone

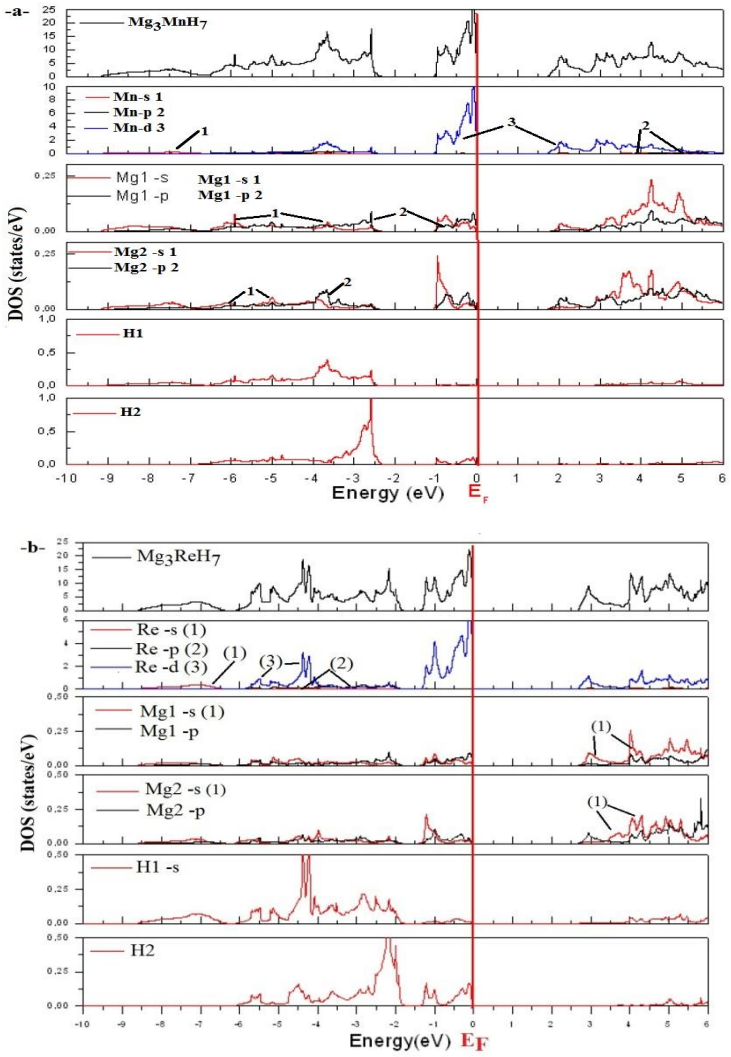

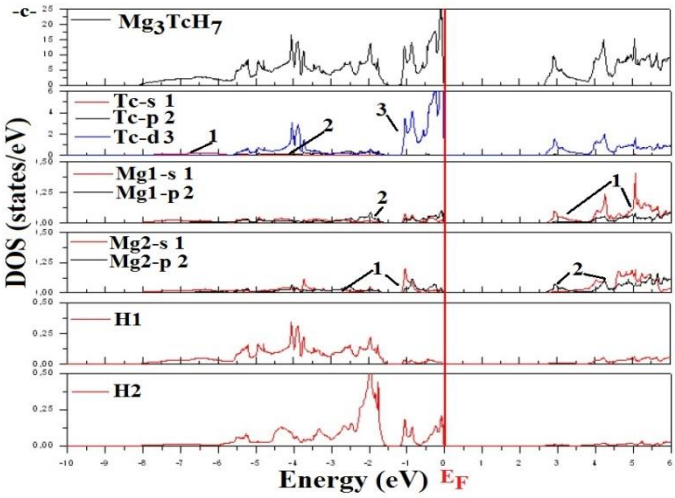

Fig. 5: The total and partial density of states of Mg_3MnH_7 -**a**, Mg_3ReH_7 -**b** and Mg_3TcH_7 -c, the Fermi level is set at zero energy and marked by the red vertical line

3.3 Optical properties

The dielectric function $\varepsilon(\omega) = \varepsilon_1(\omega) + i\varepsilon_2(\omega)$ gave an important role in determining the optical properties of matter. Where $\varepsilon_1(\omega)$ and $\varepsilon_2(\omega)$ are the real and the imaginary parts of the dielectric function, respectively. The $\varepsilon_2(\omega)$ is given as follows [24]

$$\varepsilon_2(\omega) = \frac{4\pi^2 e^2}{m^2 \omega^2} \cdot \sum_{ij} \int \left| \langle i | M | j \rangle \right|^2 (f_i(1-f_j)) \cdot \delta(E_j - E_i - h\omega) \cdot d^3k \quad (1)$$

Where M is the momentum operator, e and m are the electron charge and mass respectively. ω is the frequency of the phonon. $|i\rangle$ and $|j\rangle$ are the eingenfunctions with eigenvalues E_i and E_j respectively. f_i and f_j are the Fermi distributions for $|i\rangle$ and ($|j\rangle$ states respectively. The $\varepsilon_2(\omega)$ can be obtained using the Kramers-Krönig relation 1) [24].

$$\varepsilon_1(\omega) = 1 + \frac{2}{\pi} P \int \frac{\omega' \varepsilon_2(\omega) d\omega'}{(\omega'^2 - \omega^2)} \quad (2)$$

where P is the principal value of the integral.

All of the optical parameters such, the refractive index $n(\omega)$, the extinction coefficient $k(\omega)$, reflectivity $R(\omega)$, energy-loss $L(\omega)$ and absorption coefficient $\alpha(\omega)$ can be determined and are given as follows [25].

$$n(\omega) = \left(\frac{\varepsilon_1(\omega)}{2} + \frac{\sqrt{\varepsilon_1(\omega)^2 + \varepsilon_2(\omega)^2}}{2} \right)^{1/2} \quad (3)$$

$$k(\omega) = \left(\frac{\sqrt{\varepsilon_1(\omega)^2 + \varepsilon_2(\omega)^2}}{2} - \frac{\varepsilon_1(\omega)}{2} \right)^{1/2} \quad (4)$$

$$R(\omega) = \left(\frac{\sqrt{\varepsilon_1(\omega) + i\varepsilon_2(\omega)} - 1}{\sqrt{\varepsilon_1(\omega) + i\varepsilon_2(\omega)} + 1} \right)^2 \quad (5)$$

$$k(\omega) = \frac{\varepsilon_2(\omega)^2}{(\varepsilon_1(\omega)^2 + \varepsilon_2(\omega)^2)} \quad (6)$$

$$\alpha(\omega) = \frac{\sqrt{2}\,\omega \left(\sqrt{\varepsilon_1(\omega)^2 + \varepsilon_2(\omega)^2} - \varepsilon_1(\omega) \right)^{1/2}}{c\varepsilon_2(\omega)} \quad (7)$$

The imaginary and real parts of the dielectric function for the energy range between 0 and 20 eV of the ternary complex hydrides Mg_3MnH_7, Mg_3ReH_7 and Mg_3TcH_7 are plotted and shown in figure 6-**a**, 6-**b** and 6-**c** respectively. The imaginary parts exhibit 5 important structures (peaks) labelled A_1 (2.37 eV), A_2 (3.54 eV), A_3 (5.16 eV), A_4 (5.89 eV) and A_5 (6.86 eV), 5 peaks labelled B_1 (3.36 eV), B_2 (4.40 eV), B_3 (5.28 eV), B_4 (6.16 eV) and B_5 (7.21 eV) and 4 peaks C_1 (3.20 eV), C_2 (4.40 eV), C_3 (6.08 eV) and C_4 (6.81 eV) for Mg_3MnH_7, Mg_3ReH_7 and Mg_3TcH_7 respectively, from the range 0 to 10 eV and are shown in **Table 3**.

These peaks are the result of electronic transitions between the valence and conduction bands states, we noted that a peak does not correspond to a single transition it might be the energy transition corresponds to the same peaks. In order to identify these peaks, we decompose the optical spectrum to its contributions from each pair of valence vi and conduction cj bands [26]. The first critical point in the curve, which is attributed to the threshold for the direct optical transition $M \rightarrow M$ between the valence bands maximum and the conduction bands minimum occurs around 1.65 eV, 2.68 eV and 2.66 eV for Mg_3MnH_7, Mg_3ReH_7 and Mg_3TcH_7 respectively.

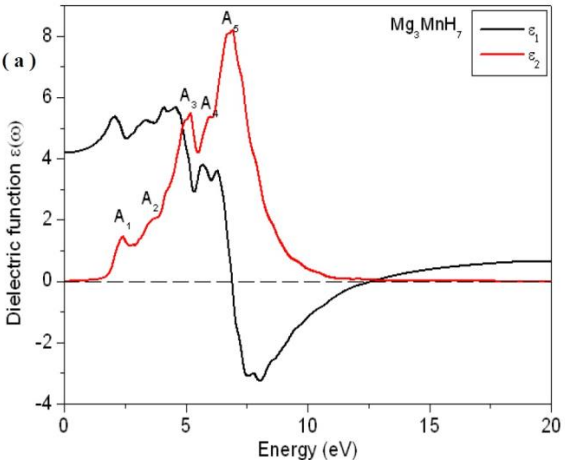

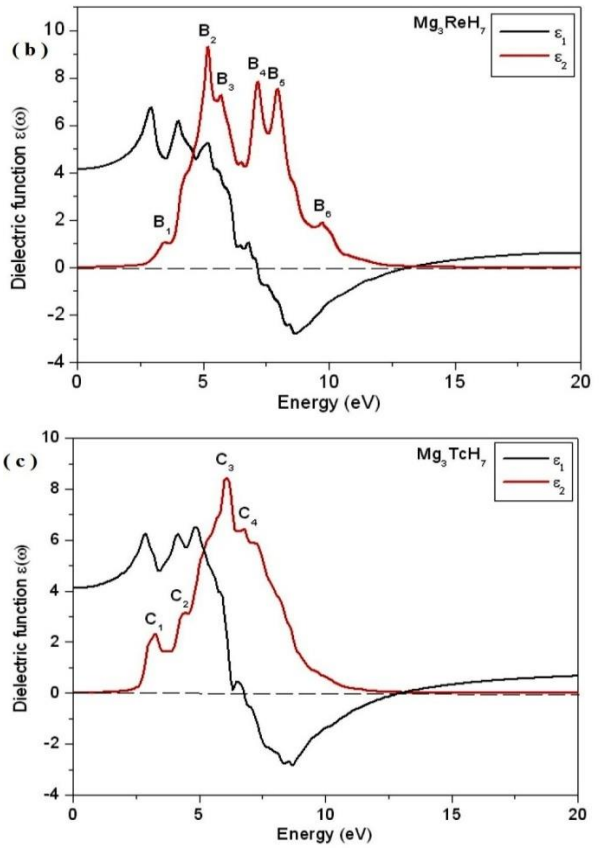

Fig. 6: The real part and imaginary part of the dielectric function of Mg_3MnH_7 **a)**, Mg_3ReH_7 **b)** and Mg_3TcH_7 **c)**

Table 3: Optical interband transitions in Mg_3MnH_7, Mg_3ReH_7 and Mg_3TcH_7

Peak position and energy (eV)		The dominant transitions	
		Transition	Energy (eV)
Mg_3MnH_7			
A_1	2.37	v4-c2	2.37
A_2	3.54	v6-c1	3.52
A_3	5.16	v8-c1	5.19
		v7-c1	5.17
A_4	5.89	v11-c2	5.80
A_5	6.86	v8-c8	6.87
Mg_3ReH_7			
B_1	3.36	v1-c2	3.36
B_2	4.40	v2-c5	4.41
B_3	5.28	v2-c7	5.29
B_4	6.16	v7-c3	6.14
B_5	7.21	v13-c2	7.22
Mg_3TcH_7			
C_1	3.20	v1-c1	3.20
C_2	4.40	v2-c3	4.40
C_3	6.08	v8-c4	6.12
C_4	6.81	v14-c1	6.86

The optical inter-band transition for Mg_3TH_7 (T=Mn, Tc, Re) are summarized in **Table 3**.

For the first complex Mg_3MnH_7 hydrides, the peaks A_1, A_2 and A_5 positioned at 2.37 eV, 3.52 eV and 6.87 eV respectively originate mainly from transition between H(2) and Mg(1)-s. Whereas, the peaks A_3 and A_4 positioned at 5.17 eV and 5.80 eV correspond to the transition from H(1) to Mn -d. In the spectrum of second complex Mg_3ReH_7 hydrides, the main peaks B_1 and B_4 at 3.36 eV and 6.14 eV respectively mainly arises from the transition between H(2) and Mg(1)-s. The peaks B_2, B_3 and B_5 positioned at 4.41 eV, 5.29 eV and 7.22eV corresponds to the transition resulting between H(1) and Re-d.

For the third complex hydrides Mg_3TcH_7 the peak C_1 positioned at 3.20 eV corresponds to the transition H(2) to Mg(1) –s, the main peaks C_2, C_3 and C_4 at 4.40 eV, 6.12 eV and 6.86 eV respectively, correspond to the transition H(1) to Tc-d. The values of static dielectric constants at the equilibrium lattice constant are 4.293, 4.157 and 4.122 for Mg_3MnH_7, Mg_3ReH_7 and Mg_3TcH_7 respectively.

In other hand, the calculated refractive index and the extinction coefficient for Mg_3TcH_7 (T=Mn, Tc and Re) in the energy range from 0 to 40 eV are displayed in figure 7-a-, 7-b-, 8-a-, 8-b- and 9-a-, 9-b-). The static refractive indices are found to have the values 2.072, 2.038 and 2.030 for Mg_3MnH_7, Mg_3ReH_7 and Mg_3TcH_7 respectively. In addition, at low frequency there exist a simple relation between n, ε_1 and ε_2, namely $n(0) = \sqrt{\varepsilon_1(0) + \varepsilon_2(0)}$ [25]. From our results you can see that obtained refractive index's are in good agreement and satisfy the relationship, indicating that our calculations are reasonable.

Figure 7-**c**, 8-**c** and 9-**c**, show the calculated reflectivity, we can see that indicates maximum value of approximately 83 % for an energy of 11.21 eV, 81 % at 11.93 eV and 82 % at 12.25 eV from Mg_3MnH_7, Mg_3ReH_7 and Mg_3TcH_7 respectively. The static reflectivity coefficient $R(0)$ is 0.122 for Mg_3MnH_7, 0.116 for Mg_3ReH_7 and 0.1156 for Mg_3TcH_7. The energy-loss spectrum $L(\omega)$ is an important factor describing the energy loss of a fast electron traversing in a material [27, 28] and are shown in figure 7-**d**, 8-**d** and 9-**d**. We can see a peak of Mg_3MnH_7, Mg_3ReH_7 and Mg_3TcH_7 at 12.57 eV, 13.13 eV and 12.89 eV respectively. These later corresponding to ω_p is generally called plasma frequency, which occurs at $\varepsilon_2(\omega) < 1$ and $\varepsilon_1(\omega) = 0$. These value correspond to the intersection between $\varepsilon_2(\omega)$ and $\varepsilon_1(\omega)$ curves in figure 6**a)**, 6**b)** and 6**c)**, when and equal to zero.

Finally, the calculated absorption coefficient is displayed in figure 7**e-**, 8**e-** and 9**e-**. We can see that the fundamental edges start from 1.58 eV, 2.60 eV and 2.50 eV for Mg_3MnH_7, Mg_3ReH_7 and Mg_3TcH_7 respectively, which are consistent with the variation of band gaps variation at the M-symmetry point in the Brillouin zone, and has main peaks at 7.44 eV, 8.73 eV and 8.60 eV for Mg_3MnH_7, Mg_3ReH_7 and Mg_3TcH_7 respectively. We can also see that the absorption coefficient increases rapidly when the energy is higher than the absorption edge, which is the typical characteristic of semiconductors and insulator.

We hope that our calculated values serve as a theoretical basis for the experiment in the future of the hexagonal Mg_3MnH_7, Mg_3ReH_7 and Mg_3TcH_7 complex hydrides.

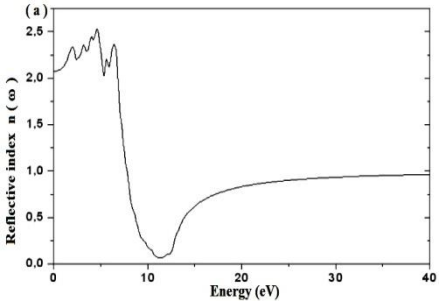

Refractive index n (ω)

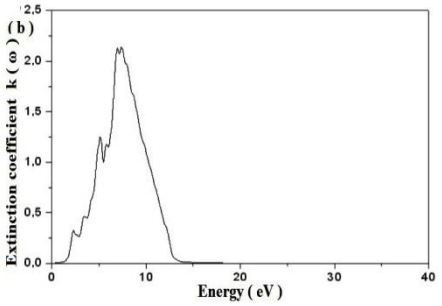

Extinction coefficient k (ω)

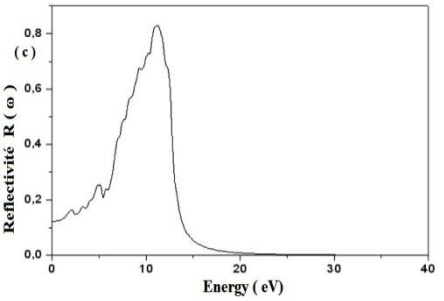

Reflectivity R (ω)

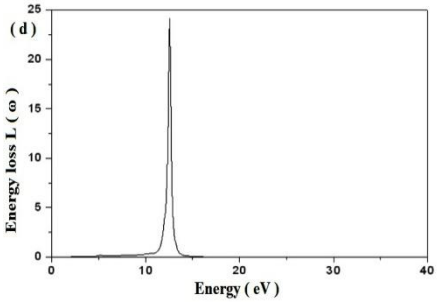

Energy-loss function L (ω)

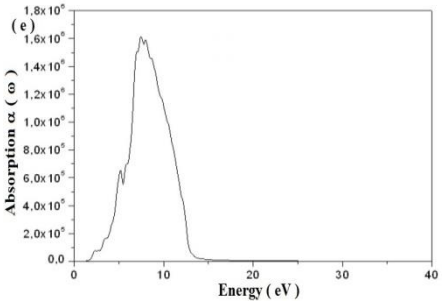

absorption coefficient α (ω)

Fig. 7: The calculated optical properties: refractive index, extinction coefficient, reflectivity, energy-loss function and absorption coefficient for Mg_3MnH_7

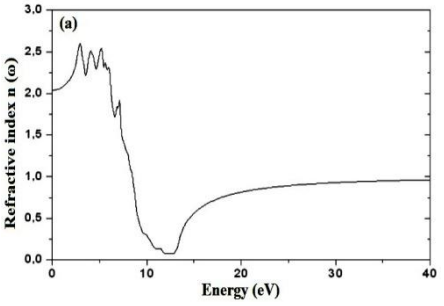

Refractive index n (ω)

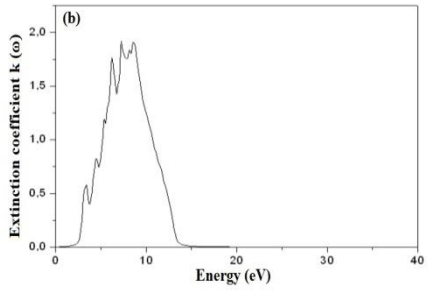

Extinction coefficient k (ω)

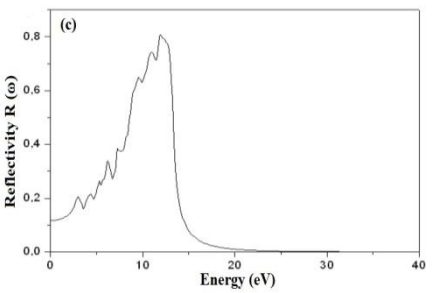

Reflectivity R (ω)

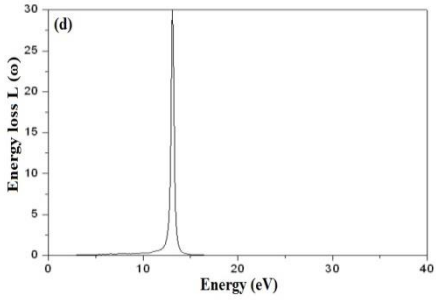

Energy-loss function L (ω)

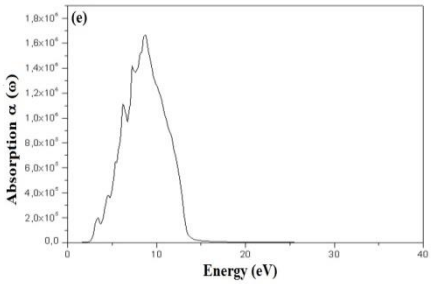

Absorption coefficient α (ω)

Fig. 8: The calculated optical properties: refractive index, extinction coefficient, Reflectivity, energy-loss function and absorption coefficient for Mg_3ReH_7.

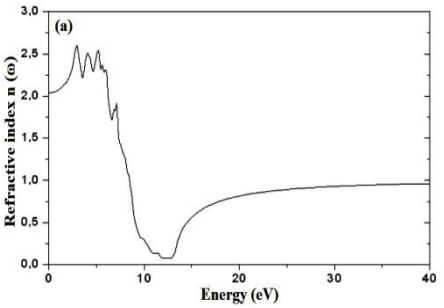

Refractive index

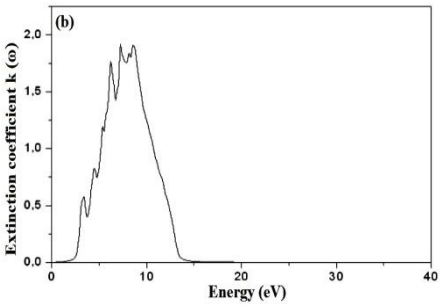

Extinction coefficient

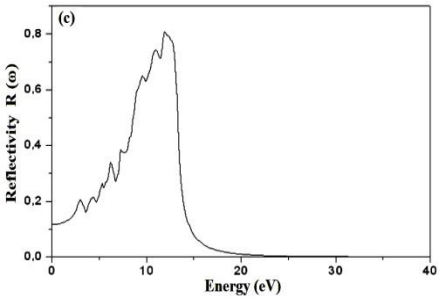

Reflectivity

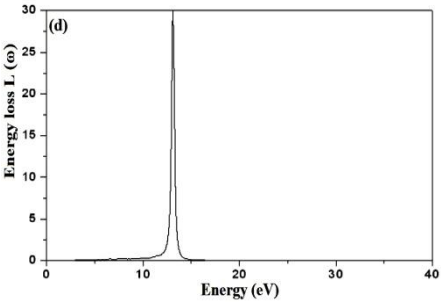

Energy-loss function L (ω)

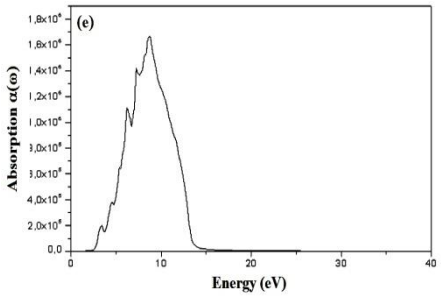

Absorption coefficient α (ω)

Fig. 9: The calculated optical properties: refractive index, extinction coefficient, reflectivity, Energy-loss function and absorption coefficient for Mg_3TcH_7

3.4 Elastic constants

The knowledge the elastic constants of the solid are very important, they can build a strong link between the mechanical, physical and crystals behaviors, they also enables measured the resistance of crystal applied stress [29-31]. For the tetragonal structure there are six independent elastic constants (C_{11}, C_{12}, C_{13}, C_{33}, C_{44}, C_{66}) and five independent elastic constants (C_{11}, C_{12}, C_{13}, C_{33}, C_{44}), since $C_{66} = (C_{11}-C_{12})/2$ for the hexagonal structure. The predicted elastic constants C_{ij} by applying the strain energy-strain curve method [32] are summarized in **Table 4**. For MgH_2, the obtained elastic constants are in good agreement with the other theoretical values [33]. From Table 4, we can see that the values of C_{11} and C_{33} for the three hexagonal structures of complex hydrides compounds Mg_3TH_7 (T=Mn, Tc and Re) are very large, suggesting that it is hard to be compressed under the uniaxial stress along the X or Z axes. Else, C_{33} is larger than C_{11}, which mean that X axis is more compressible than the Z axis for Mg_3MnH_7, Mg_3TcH_7 and Mg_3ReH_7 .

The independent elastic constants should satisfy the Born criteria [34] given by: $C_{11}>0$, $C_{33}>0$, $C_{44}>0$, $C_{66}>0$; $C_{11}-C_{12}>0$; $C_{11}+C_{33}-2C_{13}>0$; $2C_{11}+C_{33}+2C_{12}+4C_{13}>0$, for the tetragonal structure, and $C_{11}>0$, $C_{11}-C_{12}>0$, $C_{44}>0$, $(C_{11}+C_{12})C_{33}-2C_{13}^2>0$, for the hexagonal structure. From **Table 4**, we can be seen that all C_{ij} are positive and satisfy Born criteria, suggesting that the tetragonal MgH_2 and hexagonal Mg_3TH_7 (T=Mn, Tc, Re) are mechanically stable at ambient pressure.

According to Voigt-Reuss-Hill (VRH) approximation [35-39], bulk modulus (B), shear modulus (G), Young's modulus (E) and Poisson's ratio (ν) for tetragonal and hexagonal compounds were also calculated and listed in **Table 4**. The calculated bulk moduli from elastic constants are in accordance with those obtained from equation of states 'EOS'. The bulk modulus (B) and shear modulus (G) are measure of resistance to volume changes by applied pressure and to reversible deformation, respectively [40]. The obtained bulk moduli of the three complex hydrides Mg_3TH_7 (T=Mn, Tc, Re) are higher than that of MgH_2, it can be concluded that the complex hydrides have stronger resistance to volume change by applied pressure. Also, the large shear modulus and large C_{44} is an indication of more pronounced directional bonding between atoms [41]. The

obtained shear moduli of the three complex hydrides Mg_3TH_7 (T=Mn, Tc and Re) are higher and exhibits large C_{44} than that of MgH_2. These results revealed that the directional bonding in Mg_3TH_7 (T=Mn, Tc and Re) would be much stronger than that in MgH_2.

Table 4: The calculated elastic constants (in GPa), the bulk modulus (in GPa), the shear modulus (in GPa) for polycrystalline (MgH_2 and Mg_3TH_7, T=Mn, Tc, Re) within Voigt, Reuss and Hill's approximations, Young's modulus (in GPa), Poisson's ratio, and B/G ratio.

Parameter	MgH_2	Mg_3MnH_7	Mg_3TcH_7	Mg_3ReH_7
C_{11}	69.37 74.4[a]	150.29	153.78	161.68
C_{12}	36.67 38.8 [a]	25.21	34.72	36.85
C_{13}	34.48 31.4 [a]	48.04	57.64	59.22
C_{33}	143.38 136.0 [a]	209.35	206.20	215.85
C_{44}	42.62 37.6 [a]	87.03	82.20	86.93
C_{66}	52.08 53.0 [a]	62.54	59.53	62.41
B_V	54.82 54.31[b]	83.61	90.42	94.42
B_R	50.32 51.04 [b]	79.91	87.01	91.11
B_H	52.57 52.68 [b] 54.20 [a]	81.76	88.72	92.77
G_V	39.23 39.48 [b]	73.23	69.04	72.85
G_R	32.69 33.24 [b]	70.85	66.88	70.56
G_H	35.96 36.36 [b] 37.80 [a]	72.04	67.96	71.71
E	87.85 88.64 [b] 92.10 [a]	167.05	162.41	171.04
ν	0.221 0.21 [b] 0.22 [a]	0.159	0.195	0.193
B/G	1.46	1.13	1.31	1.29

[a] Ref. [33],[b] Ref. [42]

The ductile or brittle nature of materials is calculated from ratio (B/G) [11, 40, 41]. The critical number which divides ductile and brittle materials is 1.75. If $B/G > 1.75$, the material behaves in a ductile manner, otherwise a brittle manner. From **Table 4**, it is found that the MgH_2 and Mg_3TH_7 (T=Mn, Tc and Re) have a B/G ratio less than 1.75, these materials will behave in a brittle manner.

Young's modulus (E) is defined as the ratio between stress and strain, and it is used to provide a measure of the stiffness of solid, i.e., the larger the value of Young's modulus (E) correspond to the stiffer material [43]. From **Table 4** the Young's modulus (E) of Mg_3MnH_7, Mg_3TcH_7 and Mg_3ReH_7 are larger than that of MgH_2. Therefore, all ternary complex hydrides Mg_3TH_7 (T=Mn, Tc and Re) are the stiffest than MgH_2.

The value of Poisson ratio (ν) is indicative of the degree of directionality for the covalent bonds [44, 45]. For covalent materials, the value of ν is typically 0.1, for ionic materials ν is about 0.25 [46]. In this study, the calculated Poisson's ratio for MgH_2, Mg_3MnH_7, Mg_3TcH_7 and Mg_3ReH_7 compounds is 0.221, 0.159, 0.195 and 0.193 respectively, we can see that these values are greater than 0.1 and lower than 0.25, which

indicates a mixed ionic and covalent contribution. In other hand, Poisson's ratio can be generally used to characterize the ductility or brittleness for the material [47, 48]. If $\nu < 1/3$; the material behaves in a brittle manner, otherwise ($\nu > 1/3$) the material a ductile manner. From the results reported in **Table 4**, Poisson's ratio values are consistent with estimated by Pugh criteria (B/G).

3.5 Elastic Anisotropy

In order to provide the most accurate elastic study for the three complex hydrides, it is important to determine the different anisotropy parameter. Based on the calculated elastic constants, shear anisotropic factors, anisotropy of the linear bulk modulus and the percentage of anisotropy in compressibility and shear were determined and summarized in **Table 5**.

The shear anisotropic factors in the hexagonal phase can explain by three factor s.

$$A_{\{10\bar{1}0\}} = \frac{4C_{44}}{(C_{11} + C_{33} - 2C_{13})} \tag{8}$$

For the $\{01\bar{1}0\}$ shear planes between $< 10\bar{1}1 >$ and $<0001>$ directions it is.

$$A_{\{01\bar{1}0\}} = \frac{4C_{55}}{(C_{22} + C_{33} - 2C_{23})} \tag{9}$$

Finally, for the $\{0001\}$ shear planes between $\langle 11\bar{2}0 \rangle$ and $\langle 01\bar{1}0 \rangle$ directions were also calculated as follow:

$$A_{\{0001\}} = \frac{4C_{66}}{(C_{11} + C_{22} - 2C_{12})} \tag{10}$$

The deviation of the anisotropy factors from unity is a measure of the degree of elastic anisotropy possessed by the crystal. For Mg_3TH_7 (T=Mn, Tc and Re) system, the $\{0001\}$ plane exhibited isotropy, while the $\{10\bar{1}0\}$ and $\{01\bar{1}0\}$ planes deviated from isotropy, and the values of $A_{\{10\bar{1}0\}}$ were equal to $A_{\{01\bar{1}0\}}$.

Table 5: The calculated shear anisotropic factors $A_{\{10\bar{1}0\}}$, $A_{\{01\bar{1}0\}}$, $\{0001\}$, the linear bulk modulus B_a and B_c (in GPa), and the percentage of anisotropy in the compression A_B and shear A_G (in %) of Mg_3TH_7 (T=Mn, Tc, Re)

System	$A_{\{10\bar{1}0\}}$	$A_{\{01\bar{1}0\}}$	$A_{\{0001\}}$	B_a	B_c	$1/\beta$	A_B(%)	A_G(%)
Mg_3MnH_7	1.3208	1.3208	1	199.152	404.498	2.031	2.26	1.65
Mg_3TcH_7	1.3436	1.3436	1	216.908	440.097	2.029	1.92	1.59
Mg_3ReH_7	1.3421	1.3421	1	228.811	447.480	1.955	1.78	1.60

For hexagonal crystal, the linear bulk modulus along the $a-$ and $c-$ axes can be determined by following equations [39]:

$$B_a = a\frac{dP}{da} = \frac{\Lambda}{2+\beta} \tag{11}$$

$$B_c = c\frac{dP}{dc} = \frac{B_a}{\beta} \tag{12}$$

Where

$$\Lambda = 2(C_{11} + C_{12}) + 4C_{13}\beta + C_{33}\beta^2 \tag{13}$$

$$\frac{1}{\beta} = \frac{C_{33} - C_{13}}{C_{11} + C_{12} - 2C_{13}} \tag{14}$$

The factor $1/\beta$ indicates the anisotropy of linear compressibility along the $c-$axis with respect to the $a-$axis [39]. It can be seen that B_a and B_c of these three hydrides were different and increase with increasing atomic number of the element (Mn, Tc, Re), and the values of bulk modulus of B_a are smaller than B_c, indicating that compressibility along $c-$axis is stronger than a (and b)-axis due to the anisotropy.

For the percentage of anisotropy in compressibility and shear [39], it can be estimated by the two expressions $A_B = (B_V - B_R)/(B_V - B_R)$ and $A_G = (G_V - G_R)/(G_V - G_R)$, respectively. The notation (V) and (R) designed the Voigt and Reuss approximations, respectively. The values A_B is larger than A_G, which indicates the coempression anisotropy is larger than the shear anisotropy for Mg_3TH_7 (T=Mn, Tc and Re).

3.6 Debye temperature

The Debye temperature (T_{Debye}) is a fundamental parameter for understanding thermodynamic properties of solid. By using the average sound velocity, T_{Debye} can be calculated by following equation [26],

$T_{Debye} = (h/k).\left((3n/4\pi)\left(N_A\rho/M\right)\right)^{1/3}.\nu_m$, where h is Planck's constant, k is Boltzmann's constant, N_A is Avogadro's number, ρ is the density of molecule, M is the molecular mass, n is the number of atoms in the molecule and ν_m is the average sound velocity in polycrystalline materials and is given by,

$\nu_m = \left((1/3)((2/\nu_t^3) + (1/\nu_l^3)\right)^{-1/3}$; [26], were ν_t and ν_l are the transverse and longitudinal elastic wave velocities of the polycrystalline materials and are given respectively by Navier's equation [45]:

$\nu_t = \left(G/\rho\right)^{1/2}$, and $\nu_t = \left(B + (4G/3))/\rho\right)^{1/2}$. The calculated molecular mass (M), density (ρ), transverse sound velocity (ν_t), longitudinal sound velocity (ν_l), average sound velocitiy (ν_m) and Debye Temperature (T_{Debye}) are reported in **Table 6**. The results have predicted that the T_{Debye} decreased with increasing the atomic number of the element (Mn, Tc, Re) in the sequence (T_{Debye}) Mg_3ReH_7 < (T_{Debye}) Mg_3TcH_7 < (T_{Debye}) Mg_3MnH_7 (figure 3**b-**). This shows that Mg_3ReH_7 is harder than Mg_3TcH_7 which in turn is harder than Mg_3MnH_7.

Table 6: The calculated molecular mass M (in g/mol), density ρ (in g/cm^3), the longitudinal, transverse, average sound velocity (v_l , v_t , v_m in m/s) calculated from polycrystalline elastic modulus and the Debye temperatures calculated from the average sound velocity T_{Debye} (in K)

System	M	ρ	v_l	v_t	v_m	T_{Debye}
Mg_3MnH_7	134.91	2.293	8806	5605	6162	886
Mg_3TcH_7	177.97	2.792	8013	4933	5443	762
Mg_3ReH_7	266.18	4.081	6794	4191	4624	642

4. CONCLUSIONS

The structural, electronic, optical and elastic properties of three hexagonal ternary complex hydrides namely Mg_3TH_7 (T=Mn, Tc, Re) were investigated using density functional theory 'DFT' with GGA exchange correlation. The optimized lattice parameters, atomic positions and inter atomic distance are in excellent agreement with available experimental results. The calculated electronic and band structure show that the three hexagonal Mg_3MnH_7, Mg_3ReH_7 and Mg_3TcH_7 has a direct band gap with 1.65 eV, 2.68 eV and 2.66 eV values respectively. We can see that the band gap energy is highly augmented when Mn atom is substituted by Re, but it is less pronounced when Re atom is replaced by Tc. The major optical transitions occurs between H(2) and Mg(1)-s states, H(1) and -d states of Mn, Re and Tc in Mg_3MnH_7, Mg_3ReH_7 and Mg_3TcH_7 respectively. Furthermore, the optical properties such as dielectric function, refractive index, extinction coefficient, reflectivity, energy loss function and absorption coefficient for Mg_3MnH_7, Mg_3ReH_7 and Mg_3TcH_7 are computed and discussed. The obtained elastic constants for tetragonal MgH_2 are in good agreement with other theoretical works. Also, elastic constants of hexagonal Mg_3TH_7 (T=Mn, Tc and Re) compounds were calculated and compared with those of the simplest Mg-based hydride MgH_2. From, the elastic constant results MgH_2 and Mg_3TH_7 (T=Mn, Tc and Re) compounds are mechanically stable and are the brittle in nature. We have also calculated the bulk modulus, shear modulus, Young modulus and Poisson ratio by the Voigt-Reuss-Hill (VRH) approximation. It is found that the bulk modulus in the three complex hydrides Mg_3TH_7 (T=Mn, Tc, Re) are higher than that of MgH_2 and increases from Mn to Tc to Re atom. Shear anisotropy factor, linear bulk modulus and percentage anisotropy in compressibility and shear were also determined and discussed in details. Finally, Debye temperatures of Mg_3MnH_7, Mg_3ReH_7 and Mg_3TcH_7 were calculated, it was found that T_{Debye} decreases from Mn to Tc to Re atom. Unfortunately, there are no data available in literature about mechanical and optical properties of the ternary complex hydrides Mg_3TH_7 (T=Mn, Tc and Re).

REFERENCES

[1] M. Bououdina, D. Grant and G.Walker, '*Review on Hydrogen Absorbing Materials – Structure, Microstructure, and Thermodynamic Properties*', International Journal of Hydrogen Energy, Vol. 31, N°2, pp. 177 – 182, 2006.

[2] B. Sakintuna, F. Lamari-Darkrim and M. Hirscher, '*Metal Hybride Materials for Solid Hydrogen Storage: A Review*', International Journal of Hydrogen Energy, Vol. 32, N°9, pp. 1121 – 1140, 2007.

[3] C. Liu, S. Zhang, Sh. Zhang, P. Wang and H.Tian, '*Structure, Electronic Characteristic and Thermodynamic Properties of K_2ZnH_4 Hydride Crystal: A First-Principles Study*', Journal of Alloys and Compounds, Vol. 549, pp. 30 – 37, 2013.

[4] W. Bronger and G. Auffermann, '*High-Pressure Synthesis of K_2PtH_6, a Saltlike Hybride with the K_2PtH_6 Structure*', Angewandte Chemie, Vol. 33, N° 10, pp. 1112 – 1114, 1994.

[5] M. Bortz, B. Bertheville, K. Yvon, E.R. Movlaev, N. Verbetsky and F. Fauth, '*Containing the First Dridomanganese (I) Complex*', Journal of Alloys and Compounds, Vol. 279, N°2, pp. L8 – L10, 1990.

[6] S.F. Matar, '*Transition Metal Hydrido-Complexes: Electronic Structure and Bonding Properties*', Progress in Solid State Chemistry, Vol. 40, pp. 31 – 40, 2012.

[7] B. Huang, K. Yvon and P. Fischer, '*Trimagnesium Thenium (I) Heptahybride, Mg3ReH7, Containing octahedral $[ReH_6]^{5-}$ Complex Anions*', Journal of Alloys and Compounds, Vol. 197, N°, 1pp. 97 – 99, 1993.

[8] S.F. Matar, M. Nakhl and M. Zakhour, '*Electronic Structure and Bonding of the Hybrides Mg_3TH_7 (T=Mn, Re) from First Principles*', Solid State Sciences, Vol. 14, N°5, pp. 639 – 643, 2012.

[9] P. Villars and L.D. Calvert. '*Pearson's Handbook of Crystallographic Data For Intermetallic Phases*', American Society for Metals. Metals Park. Ohio. 1986. Vols. 1–3. 3258 p.

[10] E. Orgaz and M. Gupta, '*Electronic Structure of the new manganese Ternary Hybride Mg_3MnH_7*', Journal of Alloys and Compounds, Vol. 330-332, pp. 323 – 327, 2002.

[11] Y. Bouhadda, S. Djellab, M. Bououdina, N. Fenineche, Y. Boudouma, '*Structural and Elastic Properties of LiBH4 for Hydrogen Storage Applications*', Journal of Alloys and Compound, Vol. 534, pp. 20 – 24, 2012.

[12] W. Kohn and L.J. Sham, '*Self-Consistent Equations Including Exchange and Correlation Effects*', Physical Review, Vol. 140, pp. 1133 - 1014, 1965.

[13] G. Kresse and J. Furthmuller, '*Efficient Iterative Schemes for ab initio Total-Energy Calculations Using a Plane-Wave Basis Set*', Physical Review B, Vol. 54, pp. 11169 – 11186, 1996.

[14] G. Kresse and J. Hafner, '*Ab Initio Molecular Dynamics for Liquid Metals*', Physical Review B, Vol. 47, pp. 558 – 561, 1993.

[15] G. Kresse and D. Joubert, '*From Ultra-Soft Pseudo-Potentials to the Projector Augmented-Wave Method*', Physical Review B, Vol. 59, pp. 1758 – 1175, 1999.

[16] J.P. Perdew, K. Burke and M. Ernzehof, Physical Review Letters, Vol. 77, pp. 3865, 1996.

[17] P.E. Blochl, '*Projector Augmented-Wave Method*', Physical Review B, Vol. 50, N°24, pp. 17953 – 17979, 1994.

[18] M. Methfessel and A.T. Paxton, '*High-Precision Sampling for Brillouin-Zone Integration in Metals*', Physical Review B, Vol. 40, N°6, pp. 3616, 1989.

[19] H.J. Monkhorst and J.D. Pack, '*Special Points for Brillouin-Zone Integrations*', Physical Review B, Vol. 13, N°12, pp. 5188 – 5192, 1976.

[20] K. Benyelloul and H. Aourag, '*Elastic Constants Of Austenitic Stainless Steel : Investigation By The First-Principles Calculations And The Artificial Neural Network Approach*', Computational Materials Science, Vol. 67, pp. 353 – 358, 2013.

[21] R. Yu and P.K. Lam, '*Electronic and Structural Properties of MgH_2*', Physical Review B, Vol. 37, 8730 – 8737, 1988.

[22] P. Vajeeston, P. Ravidran, B.C.Hauback, H. Fjellvag, A. Kjekshus, S. Furuseth and M. Hanfland, '*Structural Stability and Pressure-Induced Phase Transitions in MgH_2*', Physical Review B, Vol. 73, N°22, 224102-8, 2006.

[23] B. Pfrommer, C. Elsasser and M. Fahnle, '*Possibility of Li-Mg and Al-Mg Hydrides Being Metallic*', Physics Review B, Vol. 50, N°8, pp. 5089 – 5093, 1994.

[24] Y. Bouhadda, Y. Boudouma, N. Fennineche and A. Bentabet, '*Ab initio Calculations Study oft he Electronic, Optical and Thermodynamic Properties of $NaMgH_3$, for Hydrogen Storage*', Journal of Physical and Chemistry of Solid, Vol. 71, N°9, pp. 1264 – 1268, 2010.

[25] Qi-Jun Liu, Zheng-Tang Liu, Xing-Sen Che, Li-Ping Feng and Hao Tian, 'First-Principles Calculations of the Structural, Elastic, Electronic, Chemical Bonding and Optical Properties of Zinc-Blende and Rocksalt GeC', Solid State Sciences, Vol. 13, N°12, pp. 2177 – 2184, 2011.

[26] O.L. Anderson, 'A Simplified Method for Calculating the Debye Temperature from Elastic Constants', Journal of Physics and Chemistry of Solids, Vol. 24, N°7, pp. 909 – 917, 1963.

[27] S.K. Tripathy and V. Kumar, '*Electronic, Elastic and Optical Properties of $ZnGeP_2$, Semicontructor under Hydrostatic Pressure*', Material Science and Engineering B, Vol. 182, pp. 52 – 58, 2014.

[28] Jianping Long, Lijun Yang, Dongmei Li and Haichuan Chen, '*First-Principles Calculations of Structural, Electronic, Optical and Elastic Properties of $LiEu_2Si_3$*, Solid State Science, Vol. 20, N° , pp. 36 – 39, 2013.

[29] T. Chihi, M. Fatmi and A. Bouhemadou, '*Structural, Mechanical and Electronic Properties of Transition Metal Hybrides MH_2 (M = Ti, Zr, Hf, Sc, Y, La, V and Cr)*', Solid State Sciences, Vol. 14, N°5, pp. 583 – 586, 2012.

[30] X.J. Chen, Z.S. Mo, R.N.Wang, M.X. Zang, B.Y. Tang, L.M. Peng and W-J. Ding, '*Elastic and Electronic Properties of The Ti5X3 (X=Si, Ge, Sn, Pb) Compounds from First-Principles Calculations*', Journal of Solid State Chemistry, Vol. 194, pp. 127 – 134, 2012.

[31] G. Sudha Priyanga, A.T. Asvini Meenaatci, R. Rajeswara Palanichamy and K. Iyakutti, '*Structural, Electronic and Elastic Properties of Alkali Hybrides (MH: M = Li, Na, K, Rb, Cs): Ab initio Study*', Computational Materials Science, Vol. 84, pp. 206 – 216, 2014.

[32] D.C. Wallace, '*Thermodynamics of Crystals*', Wiley, 1972.

[33] A. Junkaew, B. Ham, X. Zhang and R. Arroyave, '*Ab-initio Calculations of the Elastic and Finite-Temperature Thermodynamic Properties of Niobium and Magnesium Hydrides*', International Journal of Hydrogen Energy, Vol. 39, N°28, pp. 15530 – 15539, 2014.

[34] M. Born, '*Proceedings of the Cambridge Philosophical Society: Mathematical and Physical Sciences*', Volumes 1 à 50, Editor: Cambridge Philosophical Society Vol. 36, p. 160, 1940.

[35] R. Hill, '*The Elastic Behavior of Crystalline Aggregate*', Proceedings of the Physical Society, Section A, Vol. 65, pp. 349 – 354, 1952.

[38] W. Voigt, '*Lehrbuch der Kristallphysik*', Teubner Verlag Berlin-Leipzig, 1928.

[37] A. Reuss, '*Berechnung der Fliessgrenze von Mischkristallen auf Grund der Plastizitäts Bedingung für Einkristalle*', Zeitschrift für Angewandte Mathematic und Mechanik, Vol. 9, N°1, pp. 49 – 58, 1929.

[38] J.Y. Suh, Y.S. Lee, J.H. Shim and H.M. Park, '*Prediction of Elastic Properties of Precipitation-Hardened Aluminium Cast Alloys*', Computational of Materials Science, Vol. 51, pp. 365 – 371, 2012.

[39] M-M.Wu, L. Wen, B-Y Tang, Li-M. Peng, W-J. Ding, '*First-Principles Study of Elastic and Electronic Properties of $MgZn_2$ and $ScZn_2$ Phases in Mg-Sc-Zn Alloy*', Journal of Alloys and Compounds, Vol. 506, N°1, pp. 412 – 417, 2010.

[40] S.F. Pugh, '*The London, Edinburgh, and Dublin Philosophical Magazine and Journal of Science: Series 7*', Philosophical Magazine, Vol. 45, N°367, pp. 823 – 843, 1954.

[41] P. Ravindran, L. Fast, P.A. Korzhavyi, B. Johansson, J. Wills and O. Eriksson, '*Density Functional Theory for Calculation of Elastic Properties of Orthorhombic Crystals: Application to $TiSi_2$*', Journal of Applied Physics, Vol. 84, N°9, pp. 4891 – 4904, 1998.

[42] M. Zarshenas, R. Ahmed, M.B. Kanoun, B. Ul Haq, A.R.M. Isa and S. Goumri-Said, 'First Principle Investigations of the Physical Properties of Hydrogen-Rich MgH_2', Physica Scripta, Vol. 88, N°6, 8p., 2013.

[43] M. Mattesini, R. Ahuja and B. Johansson, '*Cubic Hf_3 and Zr_3N_4: A Class of Hard Materials*', Physical Review B, Vol. 68, 184108, 2003.

[44] T. Tian, X.F. Wang and W. Li, '*Ab Initio Calculations on Elastic Properties in $L1_2$ Structure Al3X and X3Al-Type (X=Transition or Main Group Metal) Intermetallic Counpouds*', Solid State Communications, Vol. 156, p. 69 – 75, 2013.

[45] F. Kong, Y. Hu, Y. Wang, B. Wang and L. Tang, '*Structural, Elastic and Thermodynamic Properties of anti-ReO_3 Type Cu_3N under Pressure from first Principles*', Computational Materials Sciences, Vol. 65, pp. 247 – 253, 2012.

[46] J. Haines, J.M. Leger and G. Bocquillon, '*Synthesis and Design of Superhard Materials*', Annual Review of Materials Research, Vol. 31, pp. 1 – 23, 2001.

[47] A.J. Wang, S.L. Shang, Y. Du, Y. Kong, L.J. Zhang, L. Chen, D.D. Zhao and Z.K. Liu, '*Structural and Elastic Properties of Cubic and Hexagonal TiN and AIN from First-Principles Calculations*', Computational Material Science, Vol. 48, N°3, pp. 705 – 709, 2010.

[48] I.N. Frantsevich, F.F. Voronov, S.A. Bokuta, '*Elastic Constants and Elastic Moduli of Metals and Insulators Handbook*', in: I.N. Frantsevich (Ed), Naukova Dumka, Kiev, 1983.